JOURNAL OF Applied Polymer SCIENCE

Preparation and Characterization of Phase-Change Material Nanocapsules with Amphiphilic Polyurethane Synthesized by 3-Allyloxy-1,2-Propanediol

Fangli Cheng,[1] Yanyan Wei,[1] Yingying Zhang,[2] Fufang Wang,[1] Tailong Shen,[1] Chengzhong Zong[1]

[1]Key Laboratory of Rubber & Plastics, Ministry of Education, Qingdao University of Science & Technology, Qingdao 266042, China

[2]Department of Pharmaceutical Science, Guangzhou University of Chinese Medicine, Guangzhou 510006, China

Correspondence to: Y. Wei (E-mail: yywei@qust.edu.cn)

ABSTRACT: Amphiphilic polyurethane was synthesized with 3-allyloxy-1,2-propanediol as the chain extender, which had an unsaturated double bond for further reaction. It was proven that,with such a structure, the amphiphilic polyurethane not only had good ability for emulsifying phase change materials(PCM) but also was capable of forming a cross-linked shell. With the amphiphilic polyurethane synthesized in this study, paraffin or methyl stearate nanocapsules in the range of 300–600 nm in size were obtained by a simple high-speed dispersion and suspension polymerization. No extra emulsifier or dispersant was added during the preparation of the nanocapsules. Tripropylene glycol diacrylate (TPGDA) was used as a crosslinking agent for strengthening nanocapsules. The crosslinking reaction of the shell materials was investigated by the NMR technique. It was found that a network structure of shells was formed after suspension polymerization. Differential scanning calorimetry (DSC) was applied to study the phase change properties of the phase-change material nanocapsules (PCMNs). The paraffin nanocapsule was found to have a rather high encapsulation efficiency of nearly 100%, and its latent heat was able to reach 104 J/g. Thermogravimetric analysis (TGA) was used to measure the thermal stability of the PCMNs. It was indicated that the weight loss rate of PCMN decreased after encapsulated by polyurethane shells and the weight loss above 200°C decreased after adding the crosslinking agent. All of the PCMN dispersions were found to have rather good dilution stability. Besides, the dried PCMN powder was able to be redispersed into water without any additional emulsifier.
 J. Appl. Polym. Sci. 130: 1879–1889, 2013

KEYWORDS: phase change material; nanocapsule; amphiphilic polyurethane; 3-allyloxy-1,2-propanediol; redispersable

Received 13 October 2012; accepted 24 March 2013; Published online 8 May 2013

DOI: 10.1002/app.39302

INTRODUCTION

The size of a nanocapsule is usually lower than 1000 nm. The synthesis methods of nanocapsules have been extensively investigated for their potential value in many areas, such as pharmaceutical, catalysis and cosmetic applications. Recently, nanocapsule technology has been applied to encapsulate phase-change materials (PCMs) to obtain better properties, such as a lower crushing rate by pumping, higher thermal stability, lower sedimentation, and higher thermal coefficient.[1,2]

The latent functionally thermal fluid with phase change material nanocapsule (PCMN)/phase-change material microcapsule (PCMM) is a new kind of heat-storage and transfer media in air conditioning devices or temperature controlling in industry. It was proven that the heat-transfer coefficients obtained by a PCM slurry were about two to four times higher than that of a pure water flow. However, due to the poor preparation technology, the properties of PCMNs and PCMMs are far from satisfying for application in functionally thermal fluids.

Both PCMMs and PCMNs are particles composed of a core and shell structure, where PCMs are the core materials enwrapped by a shell material.[3–6] Conventional *in situ* polymerization, interfacial polyaddition, and polycondensation can be applied in the production of microcapsules. However, synthetic methods for producing microcapsules have not worked out in the synthesis of nanocapsules.[7–9] It seems that it is difficult to obtain capsules smaller than 1000 nm.

Mini-emulsion and high-speed dispersion technologies have been used to assist producing PCMNs by many researchers. Zhang et al.[10] prepared nanocapsules and microcapsules containing octadecane by *in situ* polymerization. When the stirring rate was 9000 rpm, the mean particle size decreased to 0.8–0.9 μm. It seems that high-speed mechanical dispersion was very

Applied Polymer SCIENCE

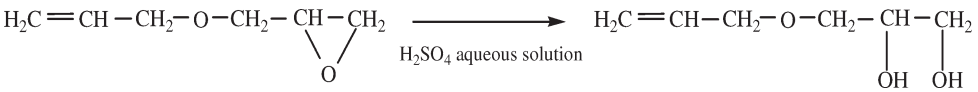

Figure 1. Hydrolyzation reaction of AGP.

limited for decreasing the nanocapsule size further. Smaller size nanocapsules can be fabricated in mini-emulsion. Luo et al.[11,12] encapsulated paraffin by mini-emulsion polymerization, and nanocapsules of about 100 nm were obtained. In Fang et al.'s[1] and Baek et al.'s[13] research, ultrasonic-assistant mini-emulsion *in situ* polymerization was used to get PCMNs ranged from 100 to 123 nm in size. The mini-emulsion *in situ* polymerization is usually applied to produce nanocapsules with polystyrene as its shell, whereas interfacial mini-emulsion polyaddition can be used to produce nanocapsules with polyurethane or polyurea shells.[14,15]

All of the methods mentioned above had a relatively complicated synthetic conditions, and a certain amount of emulsifier must be used during the synthesis and dispersion processes. The extra added emulsifier had brought other problems, such as the instability of dilution, disturbance of the rheological properties, pollution of the matrix materials, and so on.[16–18]

We have been investigating an easy and simple method for preparing PCMNs directly by suspension polymerization, and no extra emulsifier need to be added in this method. In order to achieve these goals, amphiphilic polyurethanes with 3-allyloxy-1,2-propanediol (APD) as the chain extender were synthesized and employed in our research. The common method of introducing carbon-carbon double bonds —C═C into polyurethane is using hydroxyethyl methacrylate(HEMA) to terminate the residual isocyanate group. By this method, —C═C groups are located at the end of the polyurethane chain. But APD has two hydroxyl groups in its molecular structure and it can react with polyisocyanate as a chain extender. And therefore, —C═C groups can be located in the middle of the polyurethane chain. It is possible to obtain a series of polyurethane with new kind of molecular structure by APD. The amphiphilic polyurethane synthesized in our research was found to have good emulsifying capability of emulsifying paraffine and methyl stearate in water and polyurethane itself could be a kind of shell material to participate in the suspension polymerization.[19–22] With such a polymer, no additional emulsifier need to be used during the preparation of the PCMNs.

In our research, tripropylene glycol diacrylate (TPGDA) was employed as the crosslinker for strengthening the polyurethane shell. The double bonds of polyurethane and TPGDA were reacted, and PCMNs with crosslinked polyurethane shells were formed after the reaction. PCMNs with good dilution stability and re-dispersion capability were obtained.

EXPERIMENTAL

Materials

Toluene-2,4-diisocyanate (TDI; analytically pure, Kelong Chemical) and allyl glycidyl ether (AGP; purity > 99%, Yudeheng Chemical) were used as received. 2,2-Bis(hydroxymethyl) butyric acid (DMBA; purity > 99%, Jiangxi Nancheng Hongdu Chemical Technology Development Co., Ltd.) was dried *in vacuo* at 120°C for 4 h. TPGDA (purity > 99%, Tianjin Tianjiao Chemical) was employed as a crosslinker. 1-Dodecanol (chemically pure, Bodi Chemical) was used without further purification. Dibutyltin dilaurate (analytically pure, Kelong Chemical) was used as a catalyst. Triethylamine (TEA; analytically pure, Kelong Chemical) was desiccated by molecular sieves. Solid paraffin (Shanghai Specimen Model Factory), with a melting range of 51–55°C, and methyl stearate (analytically pure, Shanghai Hengxin Chemical) were employed as PCMs.

Synthesis of APD

APD was synthesized by the following steps. First, AGP was added dropwise to a sulfuric acid aqueous solution of 15 wt % upon continuous stirring at 0°C. After the oil/water interface disappeared, the temperature of the previous solution was raised to 50°C and kept at this temperature with stirring for 1 h. Then sodium hydroxide was added to make the solution neutral. After neutralization, water was removed by vacuum distillation. In the end, sodium sulfate was separated by centrifugation, and APD was obtained. The hydrolyzation reaction of AGP is depicted in Figure 1.

Synthesis of Amphiphilic Polyurethane

The synthesis was carried out in a dry glass reactor with a stirrer, a reflux condenser, and a thermometer under a nitrogen purge. DMBA was dissolved into acetone to form a solution of 25 wt % concentration before it was added to the reactor. In the first step, 4 mol of TDI and 2 mol of DMBA were reacted at 55°C until the amount of isocyanate group was decreased to one-half of the original amount. The amount of isocyanate groups during the reaction was monitored by a dibutylamine back-titration method. Dibutyltin dilaurate was used as a catalyst with an amount of 0.1 wt % during this step. In the second step, 1 mol of APD was dropped into the reactor, and the reaction was carried on until the amount of isocyanate group was decreased to one-quarter of the original amount. In the first two steps, a series of oligomers ended with isocyanate groups was formed. In the last step, 2 mol of 1-dodecanol was charged into the reactor to block the residual isocyanate. After the disappearance of the isocyanate group, 2 mol of TEA was used to neutralize the carboxylic acid in polyurethane. The three steps of the reaction and the molecular structures are shown in Figure 2. The final polyurethane had carboxylic groups as the hydrophilic groups, the unsaturated groups for further reaction and the hydrophobic chain from 1-dodecanol.

Preparation of the PCMNs

Emulsification of the PCMs. Amphiphilic polyurethane, PCMs, and TPGDA were stirred together in a plastic cup at 50–60°C to obtain the oil phase. The formulations of the oil phase are listed in Table I. The deionized water was poured into the oil phase slowly under an agitation speed of 10,000 rpm for 5 min with a

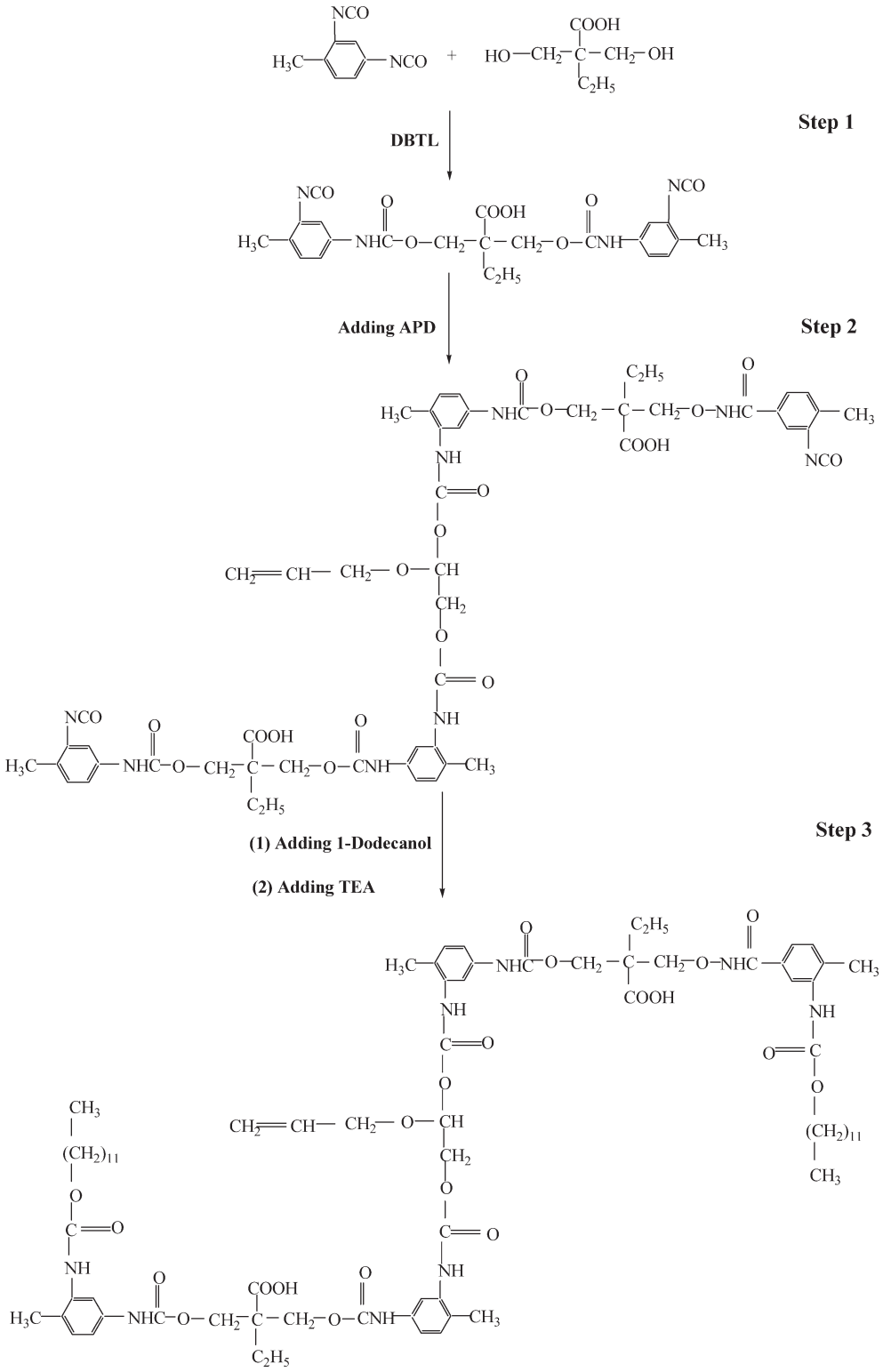

Figure 2. Synthesis of the amphiphilic polyurethane prepolymer.

FLUKO F25 homogenizer. The emulsification was maintained for 6 min. Finally, the oil materials were dispersed in water by amphiphilic polyurethane. The solid content of the dispersions was adjusted to 20 wt %.

Suspension Polymerization. The dispersion was transferred into a three-necked flask with a nitrogen purge. An ammonium persulfate aqueous solution with a 1 wt % additional amount was added to initiate the reaction. The emulsion was

Table I. Formulations of the Oil Phases and PCMNs

	Sample name					
PCM type	SP40-T20 Solid paraffin	SP50-T10 Solid paraffin	SP60-T0 Solid paraffin	MS40-T20 Methyl stearate	MS50-T10 Methyl stearate	MS60-T0 Methyl stearate
PCM (wt %)	40	50	60	40	50	60
TPGDA (wt %)	20	10	0	20	10	0
Polyurethane (wt %)	40	40	40	40	40	40

maintained at 70°C under 500 rpm of agitation for 5 h. The double bonds of polyurethane and TPGDA were reacted, and crosslinked shells of PCMNs were formed during the reaction.

After the crosslinking reaction, the dispersions were kept still at room temperature for 24 h and filtered through a sieve with a mesh diameter of 38 μm to separate the float materials; this contained the nonencapsulated materials. The obtained PCMNs dispersions were vacuum freeze dried and turned into dried powders for characterization with DSC and thermogravimetric analysis (TGA). The preparation process of the PCMNs is illuminated in Figure 3.

Characterization and Measurement

Molecular Structure. The molecular structure of the polyurethane was characterized by Fourier transform infrared (FTIR) spectroscopy–attenuated total reflectance, ^{1}H-NMR, and gel permeation chromatography (GPC). FTIR spectroscopy–attenuated total reflectance was performed on a FTIR analyzer (VERTEX 70, Bruker Co.). ^{1}H-NMR spectra of the solutions in deuterated chloroform ($CDCl_3$) were obtained with an AC-500 spectrometer (Bruker Co.). GPC was performed on an isocratic HPLC pump 1515 (Waters Co.) equipped with a refractive index detector (model 2414). The flow rate of the carrier solvent, tetrahydrofuran, was 1 mL/min, and the temperature of the columns was 30°C. The system was calibrated with a polystyrene standard.

Crosslinking Density of the PCMNs. The crosslinking density of the PCMNs was detected by a fully automatic crosslink density spectrometer (IIC MR-CDS 3500-D, IIC Co.). Before testing, the nanocapsule dispersion was freeze-dried into solid

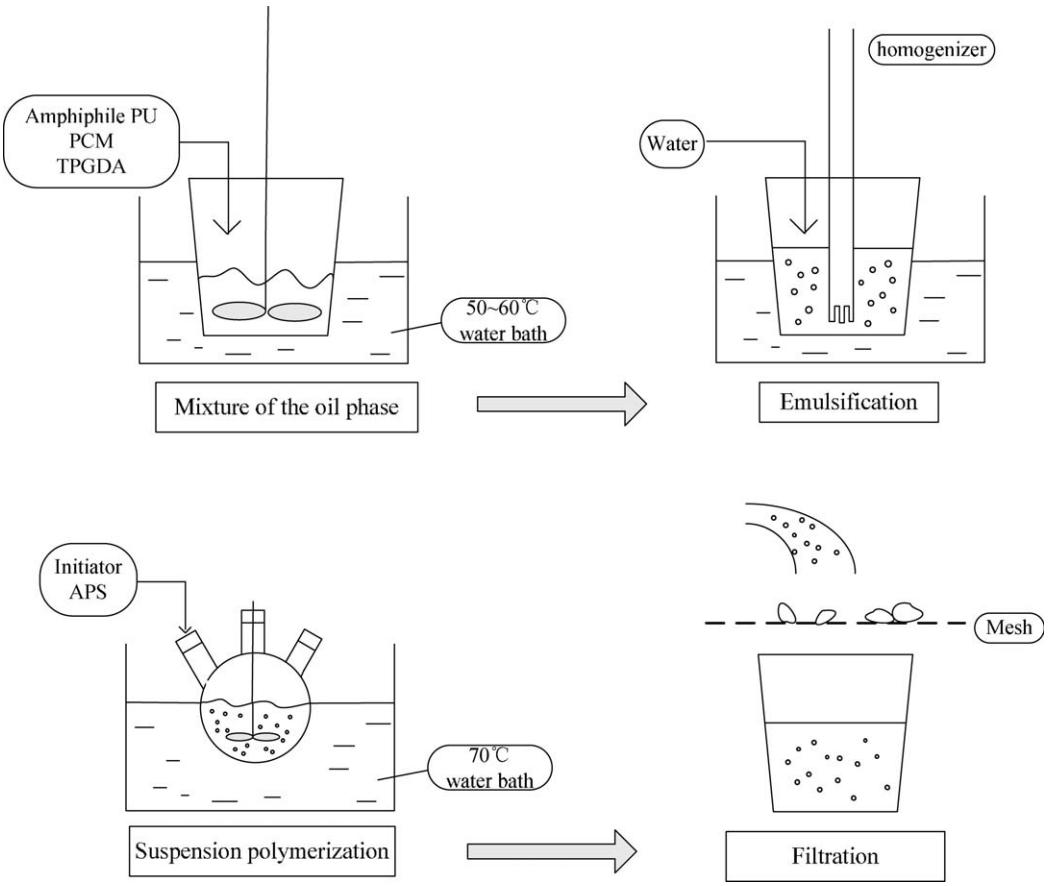

Figure 3. Scheme of the preparation steps of the PCMNs. PU, polyurethane.

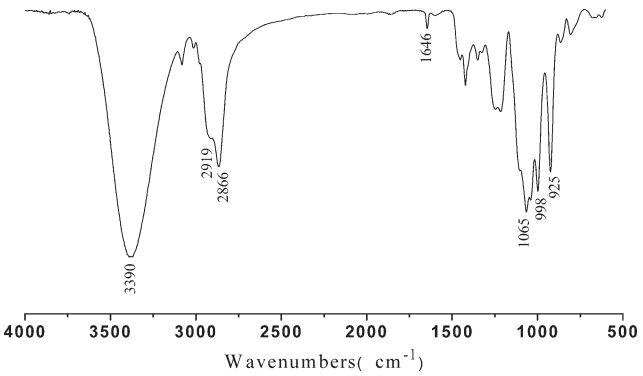

Figure 4. FTIR spectrum of the APD.

powders. The measurement provided the values of the NMR relaxation time (T_2); this correlated to the highly mobile part of the network and the relative amount of rigid and mobile fractions of the network. The measurement was performed at 100°C with a 15-MHz proton resonance frequency.

Particle Size and Morphology of the PCMNs. Quasi-elastic light scattering (Zetasizer 3000HSA, Malvern Instruments) was used to investigate the particle size and particle size distribution. The polyurethane dispersion was diluted to about 0.3% by the pure water for testing.

Transmission electron microscopy (TEM) measurements were carried out by JEM-1200EX (JEOL Co.) to observe the morphology of the nanocapsules and microcapsules. The PCMN dispersions were diluted to 0.4 wt % by distilled water. We prepared the TEM specimens by putting 1 drop of diluted emulsion on copper grids, which were dried at room temperature. After that, the TEM specimens were stained with osmium tetroxide (OsO_4) damps when placed in a special staining chamber over an OsO_4 solution at room temperature for 7 days.

Dilution Stability of the PCMN Dispersions and Redispersion Properties. After the dispersions were diluted to 1% and kept still for 4 h, the sediment and float materials were separated, dried, and weighed to evaluate the dilution stability of the PCMN dispersions.

After vacuum freeze-drying, the solid powders of the PCMNs were redispersed in water at a stirring rate of 200 rpm for 15 min. The redispersed PCMN dispersions were kept still for 3 days, and the sediment and float materials were separated, dried, and weighed to evaluate the redispersion properties.

Thermal Properties of the PCMNs. Before testing, the emulsion was turned into a solid powder by vacuum freeze drying. Differential scanning calorimetry (DSC) was performed with a DSC 204 F1 instrument (Netzsch). The solid powder sample was heated from room temperature to 100°C to eliminate the thermal history. Then, the sample was cooled down at 10 K/min from 100 to −30°C and heated at 10 K/min from −30 to 100°C in a stream of nitrogen.

TGA was performed with a TG 209 F1 instrument from Netzsch. The sample was heated at 10 K/min from 30 to 600°C in a stream of nitrogen.

RESULTS AND DISCUSSION

Molecular Structure of APD and Amphiphilic Polyurethane

APD has two hydroxyl groups as the functional groups for the chain extender. The ally group of APD provided the polyurethane with the ability to react further in suspension polymerization. In our experiments, APD was obtained by the hydrolyzation of AGP. The hydrolyzed production was characterized by IR spectroscopy (Figure 4) and H-NMR (Figure 5). In Figure 4, the absorption bands for —OH appeared at 3390 cm^{-1}; this indicated that the epoxy group was hydrolyzed into two hydroxyl groups. The peaks at about 2919 and 2866 cm^{-1} were assigned to the —CH_2— and —CH— groups, the peak at about 1065 cm^{-1} was assigned to the ether group, and the peaks at about 1646, 925, and 998 cm^{-1} were assigned to the double bond.

As shown in Figure 5, the H-NMR signals for the hydrolyzation production were assigned [$\delta = 5.791$ for H_a, $\delta = 5.067$–5.180 for H_b and H_c for the CH_2═CH— group, $\delta = 4.070$–4.210 for H_d, $\delta = 3.783$–3.906 for H_e and H_f, $\delta = 3.459$–3.582 for H_g] and are depicted in Figure 5(b). A value of $\delta = 3.361$ (H_h) was assigned to the hydroxyl group. The peak area ratio of the hydrogen shown in Figure 5(a) was calculated by $a:(b+c):d:(e+f):g:h = 1:2:2:3:2:2$; this was consistent with the molecular formula of APD illustrated in Figure 5(b). From the results of IR spectroscopy and H-NMR, it was indicated that APD was obtained by the hydrolysis of AGP.

As shown in Figure 6, the IR spectra of polyurethane revealed that the characteristic absorption band of —NCO at 2270 cm^{-1} disappeared; this indicated that the reaction of TDI was completed during the synthesis of polyurethane. The absorption band for the carbonyl group appeared at 1700 cm^{-1}, and the absorption band for —NH— appeared at 3370 and 1537 cm^{-1}, which indicated that urethane groups existed. The absorption band for —CH═CH_2 and —C—O—C— from APD appeared at 1643 and at 1067 cm^{-1}, respectively. The absorption band for —$(CH2)_n$— from 1-dodecanol appeared at 2916, 1463, and 718 cm^{-1}, respectively. The absorption band for water absorbed by carboxylic acid salt appeared at 3370 cm^{-1}. This indicated in

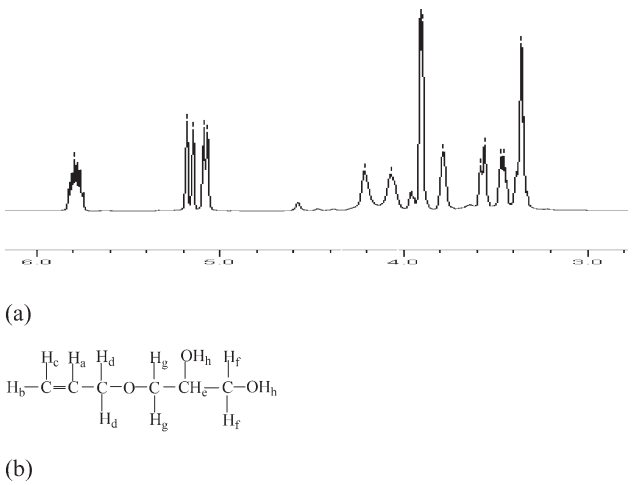

Figure 5. ^{1}H-NMR spectrum of the APD.

Applied Polymer SCIENCE

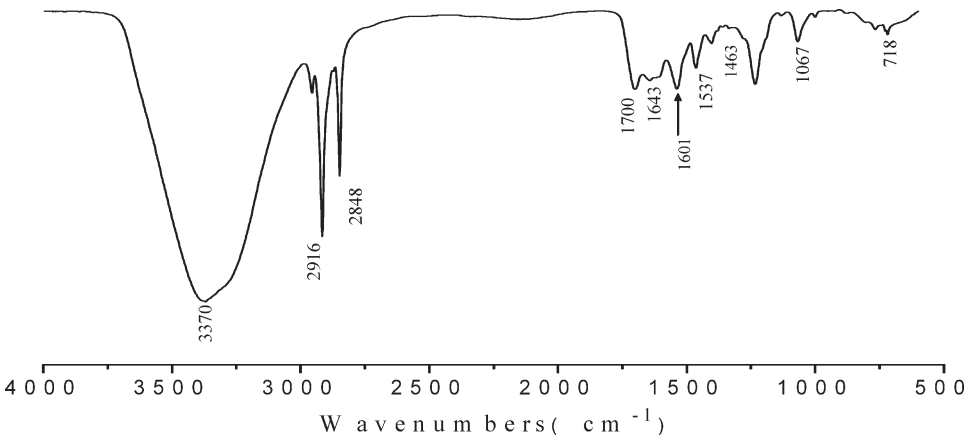

Figure 6. FTIR spectrum of the polyurethane prepolymer.

Figure 6 that the polyurethane had a chemical structure with a carboxylic group and an unsaturated group.

The molecular structure shown in Figure 2 is an ideal molecular structure, and it does not include all of the possible molecular structures. The products synthesized certainly did not have the same molecular structure presented in Figure 2. In the first step, 4 mol of TDI and 2 mol of DMBA were reacted at 55°C. Some kinds of oligomers may be produced during the reaction, such as trimers, pentamers, and heptamers. Their structures are depicted in Figure 7.

It is known that the two isocyanate groups of TDI have different reactivities: the reactivity of isocyanate in the para position is much larger than that in the ortho position, especially at such a low temperature. That is, para isocyanate has priority in reacting with the hydroxyl groups of DMBA. Therefore, we deduced that although it is possible to produce long-chain oligomers during the first step, the trimer is in the majority.

APD was dropped into the reactor in the second step to extend the chain. The low adding rate and sufficient stirring made sure that most of the APD reacted with the two oligomers. Because most of the product in the first step was trimer, there was a good chance of producing the heptamer with the structure depicted in Figure 8. In the last step, 1-dodecanol was charged into the reactor to block residual isocyanate.

Polymers, in their purist form, are mixtures of molecules of different molecular weights. It was the same with the polyurethane synthesized in our study. The number-average molecular weight was 2828, and the weight-average molecular weight was 9509, as measured by GPC. We could see the obtained polymer had a broad molecular weight distribution with a polydispersity of 3.36.

Suspension Polymerization

The amphiphilic polyurethane had a rather good ability to disperse the hydrophobic PCM stably in water. TPGDA acted as the crosslinking agent in the oil phase. The amphiphilic polyurethane, PCM, and TPGDA were dispersed into water directly by high-speed agitation. Ammonium persulfate was added in the dispersions and transferred into the droplets to initiate the polymerization of TPGDA and unsaturated double bonds in

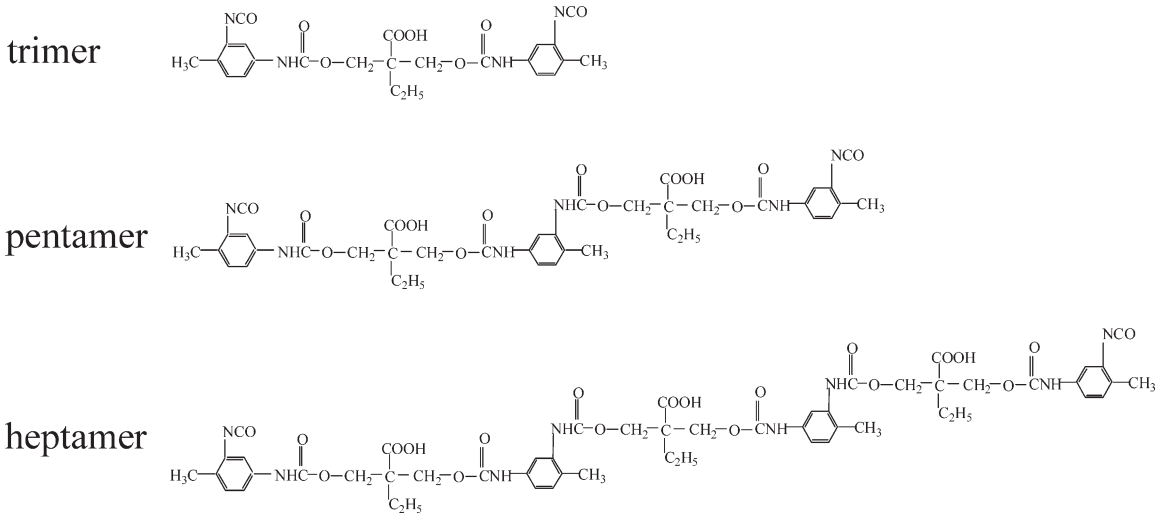

Figure 7. Molecular structure of the oligomers produced during the reaction process.

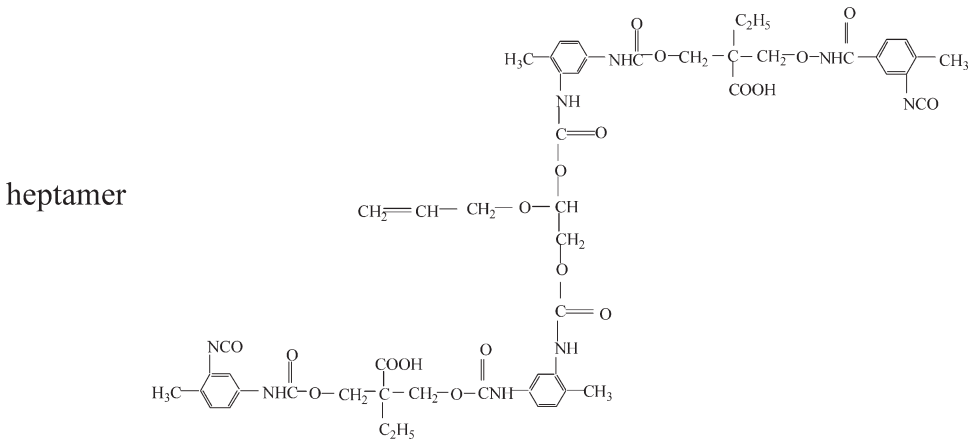

Figure 8. Molecular structure of the heptamer.

Table II. NMR Measurement Parameters of the Emulsion Particles

Reaction time (h)	A_1 (%)	T_{21} (ms)	A_2 (%)	T_{22} (ms)
0	22.38	1.06	71.69	28.75
1	41.86	0.83	49.03	17.65
2	58.64	0.44	35.86	8.48
3	60.67	0.44	34.48	8.34
5	60.68	0.45	32.39	7.48

polyurethane. Because it was a droplet nucleation system and sonication was not used, it should have been a suspension polymerization.

During the suspension polymerization, the crosslink density of the particles increased with increasing reaction time. After suspension polymerization, PCMNs with crosslinked shells were obtained. The NMR technique was used to investigate the crosslinking density of the particles at different reaction times. The data analysis yielded the relaxation time T_{21} (this correlated to the crosslinked part of the network) and T_{22} (the uncrosslinked part of the network). A_1 denoted the mass portion of the crosslinked part, and A_2 denoted the mass portion of the uncrosslinked part.

In Table II, it is shown that T21 decreased and A_1 increased with increasing reaction time, whereas T_{22} and A_2 showed an opposite changing trend. Such a measurement result showed that the crosslinking density of the particles increased with increasing reaction time. After 3 h, A_1 almost remained constant with increasing reaction time; this indicated that most of the crosslinking reaction of TPGDA and polyurethane was completed in 3 h.

Effect of the Crosslinker on the PCMN Dispersions

With sufficient carboxylic groups as the hydrophilic groups, the polyurethane could emulsify the PCMs in water. The amount of carboxylic groups in the polyurethane in our experiment was 1.33 mmol/g; this was proven to be enough to emulsify a certain percentage of oil materials to form a stable emulsion. All of the samples in Figure 9 had the same polyurethane percentage in the emulsions; this meant that the dispersed phase had the same hydrophilic group content. It is known that the hydrophilic group usually has a determinant effect on the particle size in many cases.[23] However, in our case, the average diameters of

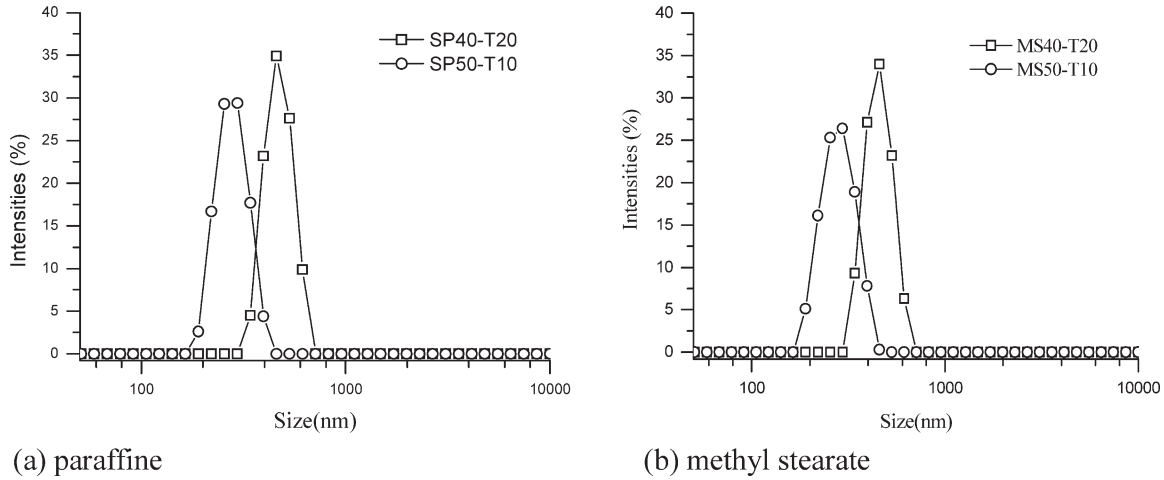

Figure 9. Particle size distributions of PCMNs with different PCMs.

Table III. Particle Sizes and Properties of the PCMN Dispersions

	Sample name			
Mean diameter	SP40-T20 651 nm	SP50-T10 300 nm	MS40-T20 605 nm	MS50-T10 278 nm
Dilution stability, coalescence collected	<1 wt %	<1 wt %	<1 wt %	<1 wt %
Redispersion properties, coalescence collected	<5 wt %	<6 wt %	<6 wt %	<5 wt %

the PCMNs showed a rather large difference; even the dispersed phases had the same content of hydrophilic groups. As is shown in Figure 9(a), the particle size of paraffin nanocapsules changed from 300 to 651 nm when the crosslinking agent increased from 10 to 20 wt %. The same phenomenon was found in nanocapsules of methyl stearate, as shown in Figure 9(b). The particle size of methyl stearate nanocapsules with 10 wt % crosslinking agent was 278 nm, whereas it increased to 605 nm when the crosslinking agent reached 20 wt %. It seemed that the percentage of crosslinking agent also had an important effect on the particle size and particle size distribution. The particle size increased, and the particle size distribution broadened with increasing crosslinking agent content. Because the TPGDA decreased the viscosity of the oil phase, it was easier for the particles to aggregate and form bigger particles and broader particle size distributions.

However, without crosslinking agent, 40 wt % polyurethane and 60 wt % methyl stearate or solid paraffin (MS60-T0 or SP60-T0) were not able to be emulsified in water to form a stable emulsion; this was due to the difficulty of mechanical stirring brought by the high viscosity. The crosslinking agent acted as a diluent during the emulsification.

Dilution Stability and Redispersion Properties after Suspension Polymerization

All of the PCMN dispersions had a rather good dilution stability. As shown in Table III, the diluted PCMN dispersions were very stable, and the coalescence collected after dilution was less than 1 wt %. The dried PCMN powders were able to be redispersed into water by simple stirring. About 5–6 wt % of the PCMNs deposited from the dispersions 3 days later after the mechanical stirring was removed. The good dilution stability and redispersion properties came from the hydrophilic groups in the polyurethane prepolymers and the crosslinked shells of the nanocapsules. With such a structure, the hydrophilic groups were fixed on the shells of the nanocapsules and could not easily escape from the surface of the nanocapsules and move into the water; even more water was added to the dispersions. The immobilized hydrophilic groups on the surface of the nanocapsules helped the dried particles to disperse into the water without extra emulsifier.

Phase-Change Properties of the PCMNs

As shown in Figure 10(a), the solid paraffin had two endothermic peaks in the DSC heating curve because it was a kind of an alkane mixture; one was at about 36°C, and the other was at about 56°C. The nanoencapsulated paraffin also had two endothermic peaks at the same temperature except that the phase-change enthalpy was lower than that of pure paraffin; this was due to the existence of polyurethane shells. The methyl stearate and encapsulated methyl stearate shown in Figure 10(b) had the similar phenomena as paraffin except that only one endothermic peak was visible in the DSC heating curve; this suggested that methyl stearate was a pure compound.

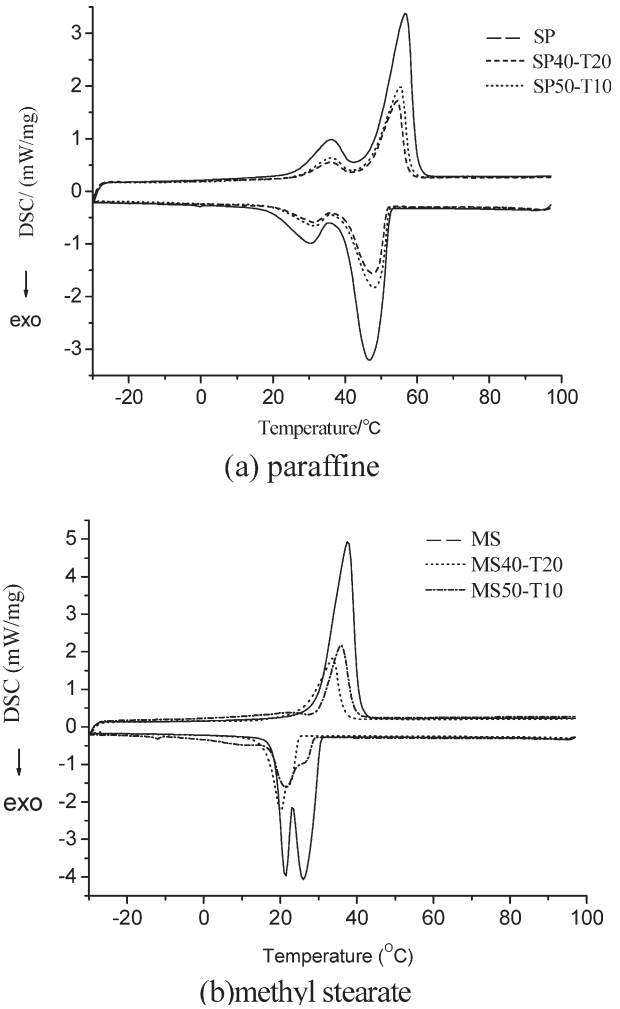

Figure 10. DSC curves of PCMNs with different PCMs.

Table IV. DSC Analysis of the PCMNs with Different PCMs

Sample	T_{m1} (°C)[a]	T_{m2} (°C)	ΔH_m (J/g)[b]	T_{c1} (°C)[c]	T_{c2} (°C)	ΔH_c (J/g)[d]	Measured PCM content (%)[e]	Calculated PCM content (%)	Efficiency of encapsulation (%)[f]
SP	36.1	56.7	198.6	30.4	46.7	198.8	—	—	—
SP40-T20	36.0	54.5	80.3	31.2	47.7	81.3	40.4	40	100
SP50-T10	36.1	55.3	102.2	31.3	48.0	104.2	51.5	50	100
MS	37.7	—	192.8	21.4	26.0	190.9	—	—	—
MS40-T20	33.7	—	71.8	20.2	22.2	68.9	37.2	40	93
MS50-T10	35.9	—	75.2	21.5	26.23	75.6	39.0	50	78

[a] T_m, peak temperature in the DSC heating curves.
[b] ΔH_m, the fusion enthalpy in the DSC heating curves.
[c] T_c, peak temperature in the DSC cooling curves.
[d] ΔH_c, crystallization enthalpy in the DSC cooling curves.
[e] Measured PCM content of SP40-T20 is equal to the ΔH_m of SP40-T20/ΔH_m of solid paraffin.
[f] Efficiency of encapsulation = Measured PCM content/Calculated PCM content.

It is shown in Table IV that the PCM content of the paraffin nanocapsules (SP40-T20 and SP50-T10) measured by DSC were consistent with the calculated ones, so the paraffin nanocapsules had a rather high efficiency of encapsulation, nearly 100%, and its latent heat was able to reach 104 J/g. This meant that the nanocapsules had a 50% mass content of PCM, although the efficiency of methyl stearate encapsulation with a 20% content of crosslinking agent was 93% and that with a 10% content was only 78%; this indicated that part of methyl stearate had not been encapsulated by the polyurethane shells. The latent heat of the nanoencapsulated methyl stearate reached 75 J/g; this was much lower than that of the paraffin nanocapsule. The content of methyl stearate in the nanocapsule of MS50-T10 was 39 wt %. It seemed that paraffin was more easily emulsified and encapsulated by the amphiphilic polyurethane (in Figure 2) than methyl stearate. Solid paraffin is a mixture of alkanes with different molecular weights. Small molecules in the paraffin decreased the viscosity of the oil phase and made the emulsification process more easy. This was probably the reason that paraffin had a higher efficiency of encapsulation than methyl stearate.

The nanoencapsulated paraffin showed the same supercooling phenomenon as bulk paraffin. Their crystallization temperature points were about 7–10°C less than the melting temperature points. The encapsulated methyl stearate and methyl stearate also had a supercooling phenomenon, and the difference between the melting and crystallization temperature points was about 9–11°C. As shown in the results of DSC, the nanoencapsulated paraffin had a lower degree of supercooling than the nanoencapsulated methyl stearate. This was because the methyl stearate was a pure compound and always had a higher supercooling degree than alkane mixtures.

Thermal Stability of the PCMNs

The TG curves of PCM, nanoencapsulated PCM, and polyurethane are shown in Figure 11. As shown in Figure 11(a), the

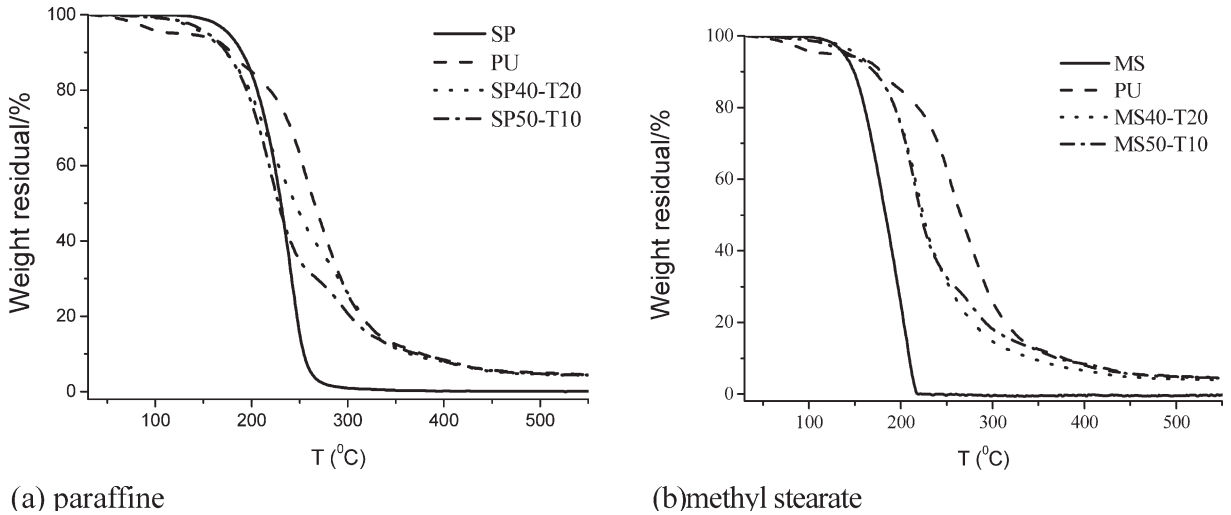

Figure 11. TGA spectra of PCMNs with different PCMs.

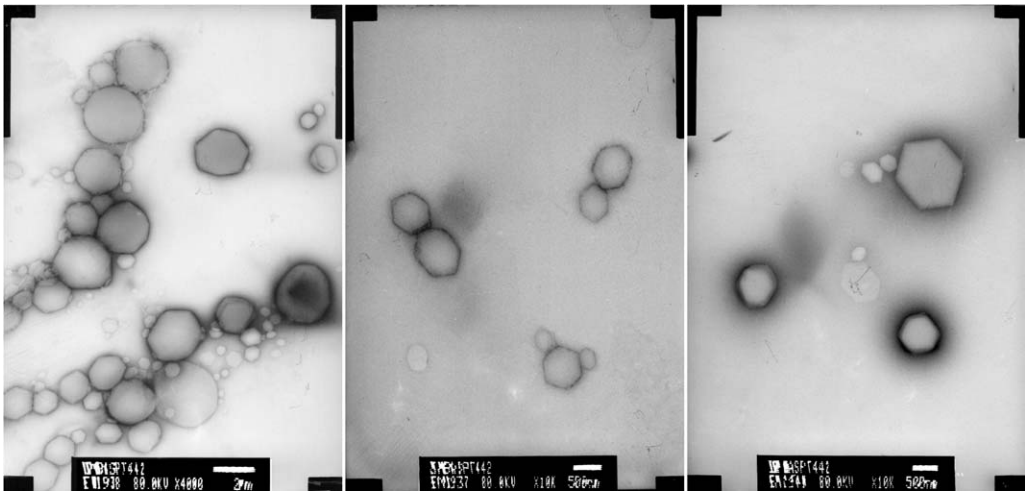

Figure 12. TEM images of the paraffin PCMNs (sample SP40-T20). The scale bars are 2 μm, 500 nm, and 500 nm from left to right.

first weight residual of SP40-T20 was 37% at 215°C, and that of SP50-T10 was 31% at 220°C. Because the first stage of weight loss was mainly contributed by paraffin, SP50-T10 with a 50% paraffin content had a larger weight loss than SP40-T20 with a 40% paraffin content. The weight loss rate of the nanocapsules decreased as the crosslinker content increased above 200°C.

The bulk methyl stearate had a sharp weight loss of nearly 100% at 207°C. The weight loss rate of methyl stearate decreased after encapsulated by polyurethane shells, as shown in Figure 11(b). MS40-T20 and MS50-T10 had smoother curves than the bulk materials.

Morphology of the PCMNs

As shown in Figures 12 and 13, most nanocapsules fell in the range of 300–1000 nm; this was consistent with the result from the particle size analyzer. It was interesting to find that most paraffin nanocapsules showed the shape of hexagon. This hexagon shape of PCMNs may have been caused by the formation of wax crystals in a limited space of nanocapsules when the temperature decreased below the melting point of paraffin. Different from paraffin nanocapsules, methyl stearate nanocapsules had an elliptical shape under TEM.

CONCLUSIONS

Amphiphilic polyurethane with APG as its chain extender was proven to have a good capability for emulsifying paraffin and methyl stearate. The shell materials were crosslinked by suspension polymerization. TPGDA was used to strengthen the shell. NMR technology was applied to investigate the crosslinking reaction during suspension polymerization. It was indicated that most crosslinking reactions of TPGDA and polyurethane were completed in 3 h. The particle size of the PCMNs increased from 300 to 600 nm, and the particle size distribution broadened when the content of TPGDA changed from 10 to 20 wt %. All of the PCMN dispersions had a rather good dilution stability and storage stability. The dried PCMNs was able to be redispersed in water, and only 5–6 wt % of the PCMNs deposited from the dispersions 3 days later. The paraffin nanocapsules had a rather high efficiency for encapsulation, nearly 100%, and their latent heat was able to reach 104 J/g. The nanoencapsulated paraffin had a lower degree of supercooling than the nanoencapsulated methyl stearate. This indicated that the amphiphilic polyurethane in the study had different emulsifying capabilities with different PCMs. The weight loss rate of the PCMNs decreased after they were encapsulated by polyurethane shells, and it decreased as the

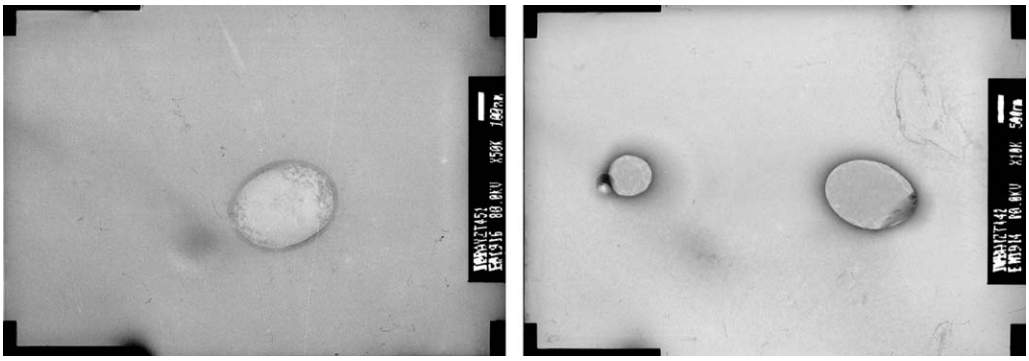

Figure 13. TEM images of the methyl stearate PCMNs (for sample MS40-T20). The scale bars are 100 and 500 nm from left to right, respectively.

crosslinker content increased above 200°C. The paraffin PCMNs had a shape of a hexagon under TEM; this was due to the formation of wax crystals in a limited space of nanocapsules.

ACKNOWLEDGMENTS

This work was supported by the National Natural Science Foundation of China (contract grant number 51103078), the Project of Shandong Province Higher Educational Science and Technology Program (contract grant number J09LB05) and the Promotive Research Fund for Excellent Young and Middle-Aged Scientists of Shandong Province (contract grant number BS2009CL020).

REFERENCES

1. Fang, Y.; Kuang, S.; Gao, X.; Zhang, Z. *Energy Convers. Manage.* **2008**, *49*, 3704.
2. Fang, G.; Li, H.; Yang, F.; Liu, X.; Wu, S. *Chem. Eng. J.* **2009**, *153*, 217.
3. Song, Q.; Li, Y.; Xing, J.; Hu, J. Y.; Marcus, Y. *Polymer* **2007**, *48*, 3317.
4. Li, W.; Zhang, X. X.; Wang, X. C.; Niu, J. *J. Mater. Chem. Phys.* **2007**, *106*, 437.
5. Zhang, H. Z.; Wang, X. D. *Colloids Surf.* **2009**, *332*, 129.
6. Sarier, N.; Onder, E. *Thermochim. Acta* **2007**, *452*, 149.
7. Jin, Z. G.; Wang, Y. D.; Liu, J. G.; Yang, Z. Z. *Polymer* **2008**, *49*, 2903.
8. Zhang, P.; Ma, Z. W.; Wang, R. Z. *Renew. Sust. Energy* **2010**, *14*, 598.
9. Inaba, H. *J. Heat Transfer* **2004**, *126*, 558.
10. Zhang, X. X.; Fan, Y. F.; Tao, X. M.; Yick, K. L. *Mater. Chem. Phys.* **2004**, *88*, 300.
11. Luo, Y. W.; Gu, H. Y. *Macromol. Rapid Commun.* **2006**, *27*, 21.
12. Luo, Y. W.; Zhou, X. D. *J. Polym. Sci. Part A: Polym. Chem.* **2004**, *42*, 2145.
13. Baek, K. H.; Lee, J. Y.; Kim, J. H. *J. Dispersion Sci. Technol.* **2007**, *28*, 1059.
14. Johnsen, H.; Schmid, R. B. *J. Microencapsulation.* **2007**, *24*, 731.
15. Gaudin, F.; Sintes-Zydowicz, N. *Colloids Surf. A* **2008**, *331*, 133.
16. Khorassani, M.; Afshar-Taromi, F.; Mohseni, M.; Pourmahdian, S. *J. Appl. Polym. Sci.* **2009**, *113*, 3264.
17. Cambiella, A.; Benito, J. M.; Pazos, C.; Coca, J.; Ratoi, M.; Spikes, H. A. *Tribology Lett.* **2006**, *22*(1), 53.
18. Ye, Q.; Xie, J.; Lu, D.; Guan, R. *Zhanjie* **2009**, *30*(12), 43.
19. Ma, N.; Li, Y.; Xu, H.; Wang, Z.; Zhang, X. *J. Am. Chem. Soc.* **2010**, *132*, 442.
20. Chai, S. L.; Jin, M. M. *Chin. J. Chem.* **2008**, *26*, 775.
21. Wei, Y. Y.; Luo, Y. W.; Li, B. F.; Li, B. G. *Colloid Polym. Sci.* **2006**, *284*, 1171.
22. Wei, Y. Y.; Xin, H. B. *E-Polymers* **2008**, *69*, 1.
23. Wei, Y. Y.; Luo, Y. W.; Li, B. F.; Li, B. G. *Colloid Polym. Sci.* **2005**, *283*, 1289.